MODELING OF ULTRASONIC NONLINEARITIES FOR DEBRIS CLOUD-INDUCED MICRO-VOIDS CHARACTERIZATION: THEORETICAL ANALYSIS AND NUMERICAL VALIDATION

Wuxiong CAO[1,2], Baojun PANG[1,*], Zhongqing SU[2], Runqiang CHI[1,*], Yuan CAI [1], Yefei HUANG [1]

[1] School of Astronautics, Harbin Institute of technology, Harbin, 150081, China

[2] Department of Mechanical Engineering, The Hong Kong Polytechnic University, Hong Kong, P. R. China

[*] Corresponding author, E-mail: pangbj@hit.edu.cn; chirq@hit.edu.cn; Tel.: 0451-86402055.

Micro-damage, from dimples through micro-voids to micro-cracks, are formed underneath the pitting damage due to the debris cloud hypervelocity impact (HVI). Evaluation of this specific type of micro-damage is far beyond the detectability of conventional approaches using guided ultrasonic waves (GUWs), because the large number of micro-voids in the pitting damage region cause highly complex. Targeting the quantitative characterization of these micro-voids, an analytical model is developed to interpret the generation of high-order modes when a GUW traversing from the perspective of linear and nonlinear GUW features. Validation of this theoretical analysis is ascertained via numerical simulation. On this basis, an evaluation framework is developed whereby the micro-voids can be quantitatively depicted.

Keywords: Debris cloud; Hypervelocity impact (HVI); Micro-voids; Guided ultrasonic wave (GUW)

1. INTRODUCTION

Over 750,000 orbiting objects sized between 1 cm and 5 cm exist in Earth's orbit, which are mingled with another ~ 170 million micrometeoroids and orbital debris (MMOD) smaller than 1 cm. Those MMOD, traveling at high speed in exceed of 2km/s, are too small to be tracked [1]. These untraceable tiny debris have posed a significant threat of HVI to the safety and integrity of all man-made spacecraft. Upon HVI, a MMOD particle larger than 1 cm is enough to penetrate any shielding layer to engender debris clouds that subsequently impinges the inner structures (e.g., pressurized module or external pressure vessel) [2], committing multitudinous pitting craters and cracks disorderedly scattered in the rear wall over a wide region, to which pitting damage is introduced. Three modalities of damage type, from dimples through micro-voids to micro-cracks, are formed underneath the pitting damage [3]. Material degradation due to the micro-voids is a potential precursor to initiate and expediate structural fragmentation and system failure.

Evaluation of this specific type of micro-damage is far beyond the detectability of conventional approaches using GUWs, because the large number of micro-voids in the pitting damage region cause highly complex, mutually-interfering wave scattering, making signal interpretation a daunting task. This has created a clear impasse to GUW-based inspection when used to detect micro-voids, let alone the quantitative characterization. Targeting the quantitative evaluation of micro-voids, a characterization strategy, associating linear with nonlinear features of GUWs, is developed. Without the need to isolate and interpret complex waves scattered by individual micro-voids in the pitting damage area.

In this paper, theoretical analysis is conducted to describe the influence of micro-voids on the propagation of Lamb wave in the pitting damaged materials. Cumulative energy transfer from fundamental to high-order harmonic modes is scrutinized using a nonlinear damage index, whereby the micro-voids can be further characterized quantitatively. To validate the theoretical analysis, numerical simulation is performed.

2. MODELING OF NONLINEARITIES IN AN ELASTIC MEDIUM

In an isotropic elastic medium, the nonlinearities in traversing GUWs mainly originate from two different sources: the material nonlinearity and the micro-damage driven nonlinearity.

2.1. Intact state

The nonlinear version of Hooke's law in and intact medium can be depicted as

$$\sigma_{ij} = (C_{ijkl} + 1/2\, M_{ijklmn}\varepsilon_{mn})\varepsilon_{kl} \tag{1}$$

where σ_{ij} denotes the stress tensor; ε_{mn} and ε_{kl} the strain tensors; C_{ijkl} the second-order elastic (SOE) tensor. M_{ijklmn} is a tensor addressing both the material nonlinearity and geometric nonlinearity, which can be expressed [4] as follows,

$$M_{ijklmn} = C_{ijklmn} + C_{ijln}\delta_{km} + C_{jnkl}\delta_{im} + C_{jlmn}\delta_{ik} \tag{2}$$

$$\begin{aligned} C_{ijklmn} = {} & \frac{1}{2}\mathcal{A}(\delta_{ik}I_{jlmn} + \delta_{il}I_{jkmn} + \delta_{jk}I_{ilmn} + \delta_{jl}I_{ikmn}) \\ & + 2\mathcal{B}(\delta_{ij}I_{klmn} + \delta_{kl}I_{mnij} + \delta_{mn}I_{ijkl}) + 2\mathcal{C}\delta_{ij}\delta_{kl}\delta_{mn} \end{aligned} \tag{3}$$

In the above, C_{ijklmn} is the third-order elastic (TOE) tensor related to material nonlinearity, while geometric nonlinearity is depicted by the last three terms of Eq. (2). δ_{ik} and such in similar forms with different subscripts are the Kronecker deltas; I_{jlmn} and such in similar form are the fourth-order identity tensors. As displayed in Eq. (3), C_{ijklmn} is directly related to three TOE constants $\mathcal{A}$, $\mathcal{B}$ and $\mathcal{C}$, which are inherent properties of material, to be obtained experimentally.

By neglecting dispersion and attenuation, the nonlinear wave equation for the GUWs in the Lagrangian coordinates is formulated as,

$$\rho\frac{\partial^2 u}{\partial t^2} = E\frac{\partial^2 u}{\partial x^2} + 2E\beta\frac{\partial u}{\partial x}\frac{\partial^2 u}{\partial x^2} \tag{4}$$

where ρ is the material density, u is the particle displacement at x along propagation direction.

In order to obtain a solution up to the 2nd order term, a perturbation theory is applied as follows,

$$u = A_1\cos(kx - wt) + A_2\cos(2kx - 2wt) \tag{5}$$

It is therefore that to calibrate the nonlinearity in the medium, a relative acoustic nonlinearity parameter β_{mat} is defined as

$$\beta_{mat} = \frac{8}{k^2 x}\frac{A_2}{A_1^2} \propto \frac{A_2}{A_1^2} \tag{6}$$

where A_2 and A_1 denote the amplitude of the second harmonic and fundamental mode, respectively.

2.2. The effect of micro-voids on propagating Lamb wave

The Rayleigh-Lamb frequency equation for symmetric and antisymmetric modes can be determined by applying the traction-free boundary condition, which results as:

$$\tan(qh)/\tan(ph) = -4k^2pq/(q^2 - k^2)^2 \tag{7}$$

$$\tan(qh)/\tan(ph) = -(q^2 - k^2)^2/4k^2pq \tag{8}$$

where $p^2 = (2\pi f/c_L)^2 - k^2$, $q^2 = (2\pi f/c_T)^2 - k^2$, $k = 2\pi f/c_P$, $2h$ denotes the thickness of plate, c_L the velocity of longitudinal wave, c_T the velocity of transverse wave, c_P the phase velocity of Lamb wave.

The Rayleigh-Lamb dispersion equation can also be depicted as $F(c, f, h, \rho, \mu, E) = 0$, which is related to the material properties, such as the density ρ, Poisson's ratio μ, elastic modulus E, and etc.

For a medium bearing pitting damage, numerous pitting craters and cracks, disorderedly scattered in the rear wall (see Figure.1(a)), accompanying with the generation of micro-voids (see Figure.1(b)), according to our previous works [3]. On top of the intrinsic material nonlinearity and geometric nonlinearity, additional sources of nonlinearities underneath the pitting damage region are introduced, mainly including the micro-voids caused acoustic nonlinearity.

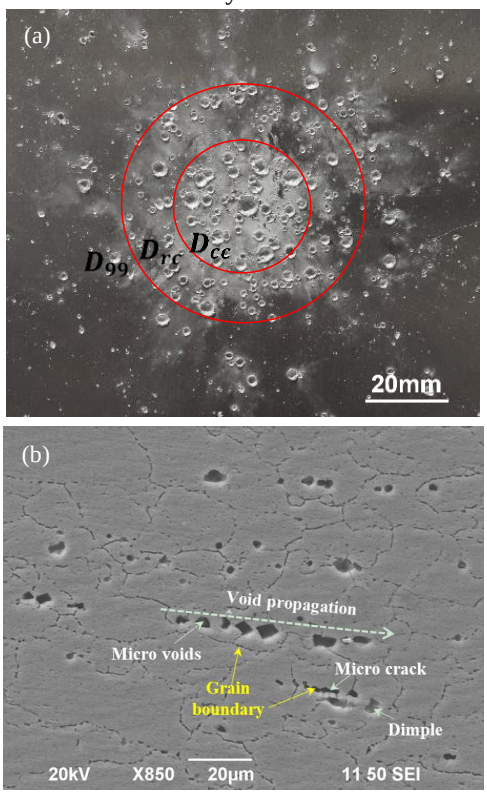

Figure 1. (a) Morphology of pitting damage induced by debris cloud HVI; (a) Microstructural damage underneath the pitting damage

In the damaged material with micro-voids, the void area fraction can be expressed as

$$f_{void} = \frac{V_{void}}{V} \times 100\% \tag{10}$$

where f_{void} is the void area fraction (for an intact solid $f_{void} = 0$), V_{void} is the void area, V is the solid area.

The effective Young's modulus and Poisson's ratio of damaged materials with micro-voids are derived using the principle of statistical continuum mechanics [5], as follows

$$E^* = \frac{E(1-f_{void})^2}{1+2\mu f_{void}} \tag{11}$$

$$\mu^* = \frac{(1/4)(4\mu + 3f_{void} - 7\mu f_{void})}{1+2f_{void} - 3\mu f_{void}} \tag{12}$$

Therefore, the velocity of longitudinal wave and transverse wave related to the elastic and physical properties of material can be expressed as,

$$c_L = \sqrt{\frac{E^*(1-\mu^*)}{\rho(1+\mu^*)(1-2\mu^*)}} \tag{13}$$

$$c_T = \sqrt{\frac{E^*}{2\rho(1+\mu^*)}} \tag{14}$$

To calculate the dispersive curve of both the intact specimen and damaged medium using the Eq.(13) and Eq.(14), as shown in the Figure 2. It can be observed that the phase velocities for all the symmetric and antisymmetric modes deceases in the damaged medium with micro-voids, leading to the mis-matching of phase velocities. As a result, the candidate mode pairs which are usually used to interrogate the debris cloud HVI-induced damage are limited.

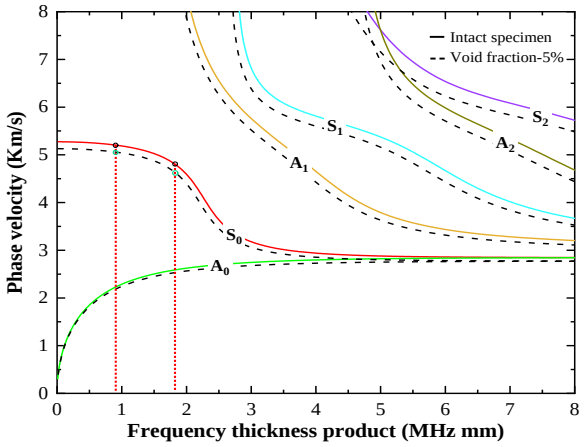

Figure 2. Phase velocity curve for Lamb wave

2.3. Generation of High Order Harmonics in GUWs due to Micro-voids

The nonlinear properties of a medium with micro-voids are mainly determined by the nonlinearity of micro-voids; the solid may be considered linear and satisfying Hooke's law.

In such a medium, the additional strain $d\varepsilon_{z'}^{'}$ occurs along the z' axis. A variation in void area $\Delta V(\varphi)$ leads to the additional strain [6], as

$$d\varepsilon_{z'}^{'} = \Delta V(\varphi) N(\varphi,\theta) \sin\varphi d\varphi d\theta \tag{15}$$

where $N(\varphi,\theta)$ is a function of the micro-voids distribution within the angles φ and θ, $N(\varphi,\theta)\sin\varphi d\varphi d\theta$ is the number of micro-voids with normal oriented in the unit area. And then the additional strains due to all micro-voids can be depicted as,

$$\varepsilon_{z'}^{'} = \frac{\sigma}{E}\left[1 + \int_0^{2\pi}\int_0^{\pi/2} N(\varphi,\theta)\sin\varphi \times \cos^4\varphi\left(a + \frac{b\sigma}{2E}\cos^2\varphi\right)d\varphi d\theta\right] \tag{16}$$

Therefore, the acoustic nonlinearity parameter associated with non-interacting micro-voids in material can be expressed as,

$$\beta_{void} \approx 5\times 10^6 N_0 R_{void}^4 \tag{17}$$

where N_0 is the concentration of micro-voids (number of micro-voids in per unit area) in the interior of the material and R_{void} is the radius of the micro-voids.

Taking about the global and local nonlinearity parameters into account, a hybrid acoustic nonlinearity parameter β_{total} is constructed in this study, as

$$\beta_{total} = \beta_{mat} + \beta_{void} \tag{18}$$

3. IMPLEMENT OF MODELING

3.1. Problem description

A dedicated modeling technique is developed and implemented using the finite element method (Abaqus/Explicit). All the effect on nonlinearities discussed in the above including the micro-voids induced nonlinearity and the effective elastic constant, are taken into account. The S0-S0 mode pair is investigated to gain an insight into the generation of second harmonic due to the intrinsic material nonlinearity and the micro-voids induced nonlinearity. The modeling of material,

geometric and micro-voids induced nonlinearities is realized by substituting the stress-strain relation in the calculation process of the Abaqus/Explicit with a specifically defined nonlinear stress-strain relation via user subroutine VUMAT.

Table 1. Physical properties of the aluminum plate

Material	*Elastic modulus (GPa)*	*Density (10^3 kg/m^3)*	*Poisson's ratio*
Aluminum 6061T	68.9	2780	0.33
	A (GPa)	***B (GPa)***	***C (GPa)***
	-320	-200	-190

Consider a plate with thickness of 3mm, the material parameters including density, Young's modulus, Poisson's ratio, and TOE constants listed in Table 1, are defined as the input variables of VUMAT. A uniform displacement of 7-cycle Hanning windowed sinusoid tone burst with a central frequency of 300kHz is applied on the left end of the plate to investigate the $S_0 - S_0$ mode pair which does not satisfy the internal resonance requirements. To warrant the accuracy of the simulation result, a fine mesh with the element length of 0.1 mm, 1/30 of the wavelength of the second harmonic S0 mode, is assigned to the whole model.

To model the micro-voids induced material nonlinearity, a series of micro-voids with the diameter of 5μm are uniform distributed, and the effective elastic constant (e.g., Young's modulus and Poisson's ratio) are considered in the localized damaged region, as shown in Figure 3.

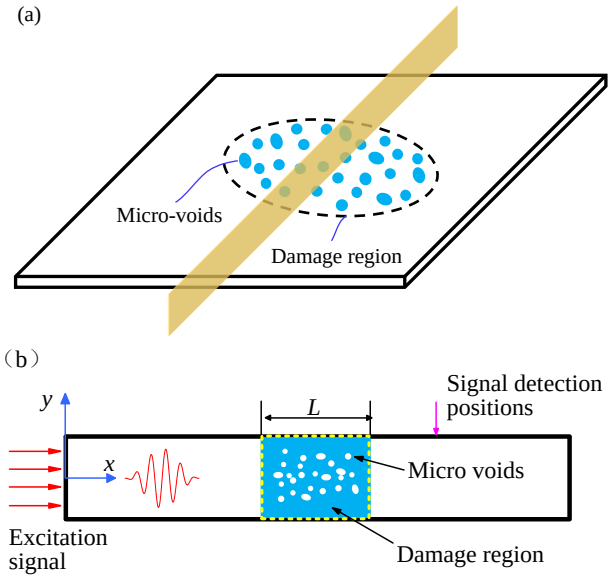

Figure 3. (a) Schematic of a plate bearing pitting damage; (b) Numerical model with micro-voids

3.2. Results and discussion

Numerical results show that the time of arrival (TOA) signal in the damage material is delayed due to the micro-voids, as shown in Figure 4. Because micro-voids can cause the reduction of linear elastic constants (e.g., Young's modulus, Poisson's ratio), leading to decrease of phase velocity.

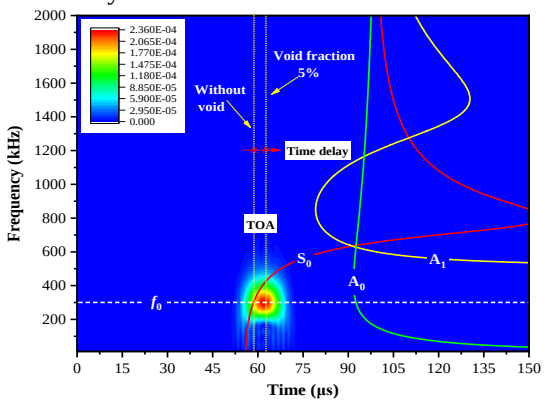

Figure 4. Wavelet transform spectrum of time-domain signal (Void area fraction 5%)

It can be seen that the low frequency thickness product of S_0 mode changes slightly, as shown in Figure 5. Variation of void area fraction will lead to the mis-matching of phase velocities, as well as the decrease of dispersion length L_n, expressed as Eq.(19).

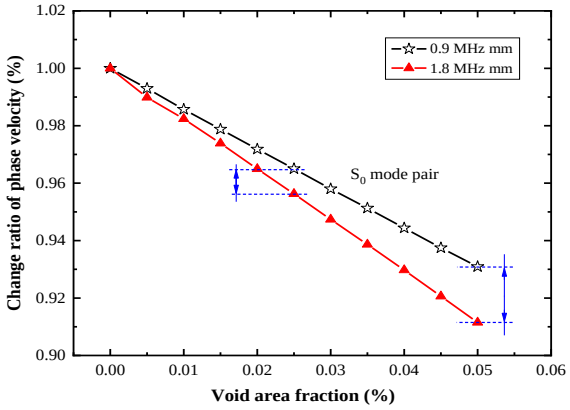

Figure 5. Changing of Lamb wave phase velocity *vs.* void area fraction

$$L_n = \frac{2\pi}{|\kappa_m - 2\kappa_a|} = \frac{1}{2f(1/c_{P-2\omega} - 1/c_{P-\omega})} \quad (19)$$

where f is the frequency of excitation signal, $c_{P-2\omega}$ is the phase velocity of double frequency, $c_{P-\omega}$ is the phase velocity of fundamental frequency.

Figure 6(a) displays the raw time-domain signal for the $S_0 - S_0$ mode pair acquired after a propagation distance of 260 mm. Extracting magnitudes of the signal at fundamental frequency and double frequency (Figure 6(b)) through STFT to calculate the total acoustic nonlinearity parameter β_{total}.

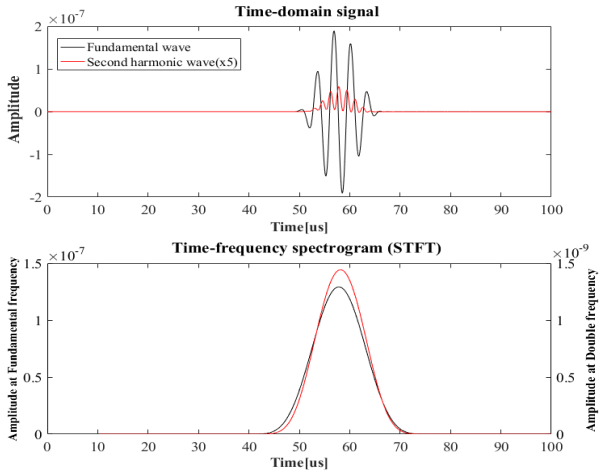

Figure 6. Signals of model pair $S_0 - S_0$ at 260 mm (Void area fraction 5%)

The quasi-matching of phase velocities, guarantees the accumulation of the second harmonic mode, as shown in the Figure 7.

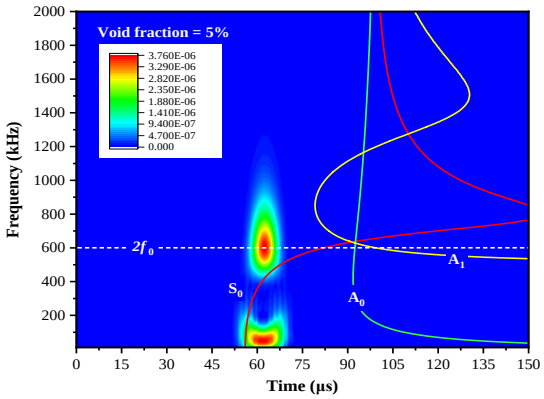

Figure 7. Wavelet transform spectrum of signal at double frequency (Void area fraction 5%)

Numerical results reveal that acoustic nonlinearity parameter accumulates gradually with the increasing of both micro-voids area fraction and width of damage region, as shown in Figure 8 and Figure 9.

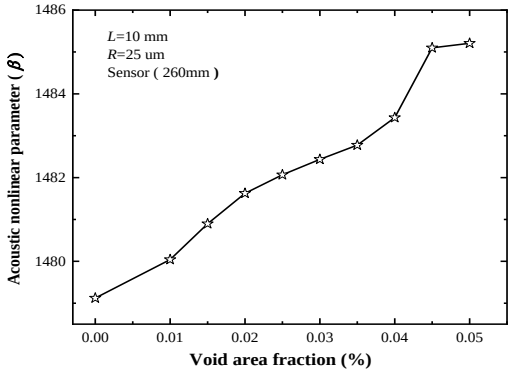

Figure 8. Nonlinear indices under different void area fraction

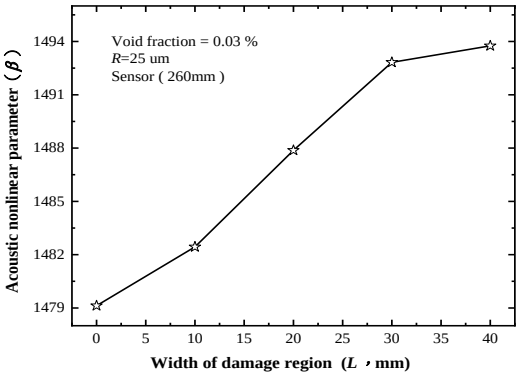

Figure 9. Nonlinear indices under different width of damage region

4. CONCLUSION

In this research, an analytical model is proposed for describing the influence of micro-voids on the acoustic nonlinearity in the pitting damaged materials. Simulation of NUWs propagation in the 6061T alloy with uniformly distributed micro-voids has been carried out. Numerical results indicate that the damage index (*DI*) developed in this research can be used to interpret the contribution of micro-voids to acoustic nonlinearities and quantitatively characterization the severity of micro-voids.

ACKNOWLEDGEMENTS

The work was supported by the Natural Science Foundation of China (No. 11772113).

REFERENCES

[1] Space.com. Tech. Available online: https://www.space.com/36602-space-junk-cleanup-concepts.html (accessed on 03 January 2019).

[2] Drolshagen, G. Impact effects from small size meteoroids and space debris. *Adv. Space Res.* 2008, 41, 1123–1131.

[3] Cao, W.X, Wang, Y.F, et al. Microstructural Characterization of Hypervelocity Debris Cloud-induced Pitting Damage in AL-Whipple Shields. *International Journal of Impact Engineering* (Submitted).

[4] Landau, L. D.; Lifshitz, E., *Theory of Elasticity, vol. 7.* Course of Theoretical Physics 1986, 3, 109.

[5] Ramakrishnan N, Arunachalam V S. Effective elastic moduli of porous solids[J]. *Journal of materials science*, 1990, 25(9): 3930-3937.

[6] Nazarov V E, Sutin A M. Nonlinear elastic constants of solids with cracks[J]. *The Journal of the Acoustical Society of America*, 1997, 102(6): 3349-3354.